International Journal of
Molecular Sciences

MDPI

Article

SARS-CoV-2 Spike Proteins and Cell–Cell Communication Induce P-Selectin and Markers of Endothelial Injury, NETosis, and Inflammation in Human Lung Microvascular Endothelial Cells and Neutrophils: Implications for the Pathogenesis of COVID-19 Coagulopathy

Biju Bhargavan and Georgette D. Kanmogne *

Department of Pharmacology and Experimental Neuroscience, College of Medicine, University of Nebraska Medical Center, Omaha, NE 68198-5800, USA; bbhargavan@unmc.edu
* Correspondence: gkanmogne@unmc.edu

Abstract: COVID-19 progression often involves severe lung injury, inflammation, coagulopathy, and leukocyte infiltration into pulmonary tissues. The pathogenesis of these complications is unknown. Because vascular endothelium and neutrophils express angiotensin-converting enzyme-2 and spike (S)-proteins, which are present in bodily fluids and tissues of SARS-CoV-2-infected patients, we investigated the effect of S-proteins and cell–cell communication on human lung microvascular endothelial cells and neutrophils expression of P-selectin, markers of coagulopathy, NETosis, and inflammation. Exposure of endothelial cells or neutrophils to S-proteins and endothelial–neutrophils co-culture induced P-selectin transcription and expression, significantly increased expression/secretion of IL-6, von Willebrand factor (vWF, pro-coagulant), and citrullinated histone H3 (cit-H3, NETosis marker). Compared to the SARS-CoV-2 Wuhan variant, Delta variant S-proteins induced 1.4–15-fold higher P-selectin and higher IL-6 and vWF. Recombinant tissue factor pathway inhibitor (rTFPI), 5,5′-dithio-bis-(2-nitrobenzoic acid) (thiol blocker), and thrombomodulin (anticoagulant) blocked S-protein-induced vWF, IL-6, and cit-H3. This suggests that following SARS-CoV-2 contact with the pulmonary endothelium or neutrophils and endothelial–neutrophil interactions, S-proteins increase adhesion molecules, induce endothelial injury, inflammation, NETosis and coagulopathy via the tissue factor pathway, mechanisms involving functional thiol groups, and/or the fibrinolysis system. Using rTFPI, effectors of the fibrinolysis system and/or thiol-based drugs could be viable therapeutic strategies against SARS-CoV-2-induced endothelial injury, inflammation, NETosis, and coagulopathy.

Keywords: SARS-CoV-2 spike proteins; human lung endothelial cells; neutrophils; P-selectin; von willebrand factor; IL-6; citrullinated histone H3; neutrophils extracellular traps; TFPI; DTNB; thrombomodulin

Citation: Bhargavan, B.; Kanmogne, G.D. SARS-CoV-2 Spike Proteins and Cell–Cell Communication Induce P-Selectin and Markers of Endothelial Injury, NETosis, and Inflammation in Human Lung Microvascular Endothelial Cells and Neutrophils: Implications for the Pathogenesis of COVID-19 Coagulopathy. *Int. J. Mol. Sci.* **2023**, *24*, 12585. https://doi.org/10.3390/ijms241612585

Academic Editors: Eliza Russu, Alexandru Schiopu and Emil Marian Arbănași

Received: 28 April 2023
Revised: 31 July 2023
Accepted: 3 August 2023
Published: 9 August 2023

1. Introduction

Severe acute respiratory syndrome coronavirus-2 (SARS-CoV-2), the causative agent of coronavirus disease 2019 (COVID-19), has so far infected over 686 million people worldwide, resulting in over 6.88 million deaths and counting [1–3]. Although SARS-CoV2-induced immunopathology can affect several organs, postmortem examination shows that for most COVID-19 patients, the primary cause of death was acute lung injury associated with the presence of virions and spike (S) proteins in lung blood vessels, endothelial injury, increases in leukocyte infiltration in lung tissues, circulating prothrombotic factors, inflammation, and thrombosis [4–7]. Endothelial injury is also associated with the release of von Willebrand factor (vWF) from endothelial granules, upregulation of adhesion molecules, increased neutrophil activation, adhesion and transmigration into vascular walls [8,9]. The pathogenesis of these pulmonary complications in COVID-19 patients is unknown.

Coronaviruses enter and infect target cells by binding their S-protein to cellular angiotensin-converting enzyme-2 (ACE2) [10,11], and human neutrophils [12,13] and endothelial cells [14–16] express ACE2. Because SARS-CoV-2 and its S-proteins are present in tissues and bodily fluids of infected patients and COVID-19 pathology includes endotheliopathy and leukocyte infiltration into the lungs [7,17,18], it is important to determine whether viral S-proteins directly contribute to these lung pathologies and whether leukocyte interactions with the vascular endothelium influence SARS-CoV-2-induced pathologies. In the present study, we investigate the direct and indirect effects of S-protein exposure on the expression and secretion of adhesion molecules, markers of endothelial injury, and inflammation. Because increased levels of neutrophil extracellular traps (NETs) are associated with COVID-19 pathology and disease severity [19–22], we also investigated the direct and indirect effects of S-protein exposure on markers of NET activation and release (NETosis). We demonstrate that exposure of primary human lung microvascular endothelial cells (HLMEC) or neutrophils to S-proteins and endothelial–neutrophil interactions induced transcription and expression of P-selectin and significantly increased the expression and secretion of vWF, interleukin (IL)-6, and citrullinated histone H3 (cit-H3), a marker of NETosis. A trend toward higher P-selectin and vWF levels and significantly higher IL-6 levels was observed with SARS-CoV-2 Delta variant S-proteins (SD) compared to Wuhan variant S-proteins (SW). Recombinant tissue factor pathway inhibitor (rTFPI; the primary physiological inhibitor of the extrinsic pathway of blood coagulation [23–26]), as well as 5,5′-dithio-bis-(2-nitrobenzoic acid) (DTNB; a thiol blocker) and thrombomodulin (TM; a high affinity thrombin receptor [27]), blocked S-protein-induced expression of vWF, IL-6, and cit-H3.

These data suggest that when the lung endothelium or neutrophils are exposed to SARS-CoV-2, viral S-proteins increase adhesion molecules and induce endothelial injury, inflammation, and NETosis via the TF pathway and mechanisms involving functional thiol groups and the fibrinolysis system. Furthermore, any of these two cell populations exposed to SARS-CoV-2 or viral S-proteins can induce injury, inflammation, and NETosis in non-exposed neighboring cells. These findings suggest that viable therapeutic strategies against SARS-CoV-2-induced cellular injury, NETosis, and inflammation could include rTFPI, effectors of the fibrinolysis system, and/or thiol-based drugs.

2. Results

2.1. Exposure of HLMEC or Neutrophils to S-Proteins and Endothelial–Neutrophil Interactions Increased P-Selectin Transcription

Compared to controls (untreated cells, cells treated with heat-inactivated S-proteins, or cells pretreated with recombinant human (rh) ACE2), exposure (6–24 h) of HLMEC to SW or SD increased P-selectin mRNA by 12- to 20-fold and 10- to 67-fold, respectively; with the largest increase (51.7- to 67-fold) observed at 12 h (Figure 1A). Co-culture of SW- or SD-treated HLMEC with neutrophils increased P-selectin mRNA in HLMEC by 64.7- to 258-fold and 138- to 650-fold, respectively (Figure 1B), and increased P-selectin mRNA in neutrophils by 17- to 92-fold and 148- to 652-fold, respectively (Figure 1C). Co-culture of SW- or SD-treated neutrophils with HLMEC increased P-selectin mRNA in HLMEC by 2.8- to 62-fold and 4- to 262-fold, respectively (Figure 1D), and increased P-selectin mRNA in neutrophils by 11- to 136-fold and 77- to 228-fold, respectively (Figure 1E).

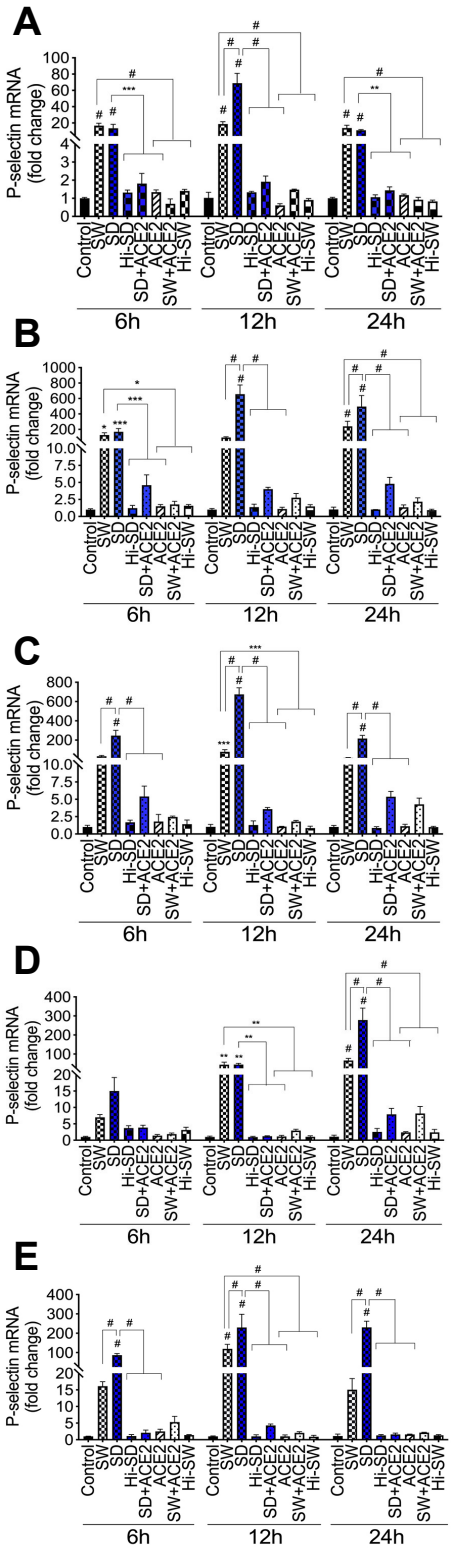

Figure 1. S-proteins and endothelial–neutrophil interactions induce P-selectin transcriptional upregulation in HLMEC and neutrophils. (**A**): HLMEC treated (for 6–24 h) with 1 nM S-protein Wuhan (SW) or Delta (SD) variants. (**B**,**C**): HLMEC were treated (6 h) with SW or SD, washed, and co-cultured (6–24 h) with neutrophils. (**D**,**E**): neutrophils treated (6 h) with SW or SD, washed, and co-cultured (6–24 h) with HLMEC. P-selectin mRNA in endothelial cells (**A**,**B**,**D**) and neutrophils (**C**,**E**) was quantified by real-time PCR. Data presented as mean ± standard deviation. Control: untreated cells; ACE2: cells treated with recombinant human (rh) ACE2 (1 µg/mL). Hi: cells treated with heat-inactivated S-proteins. * $p < 0.015$; ** $p < 0.007$; *** $p < 0.0007$; # $p < 0.0001$.

2.2. Exposure of HLMEC to S-Proteins Induced P-Selectin Expression

Immunofluorescence imaging showed that, compared to controls, exposure (12 h) of HLMEC to SW or SD increased P-selectin expression by 7- to 9-fold and by 8.9- to 11.3-fold, respectively (Figure 2A,B). Western blot analysis further confirmed these findings; compared to controls, SW and SD, respectively, increased P-selectin levels by 4.5- to 63-fold and by 6.4- to 110-fold (Figure 2C,D).

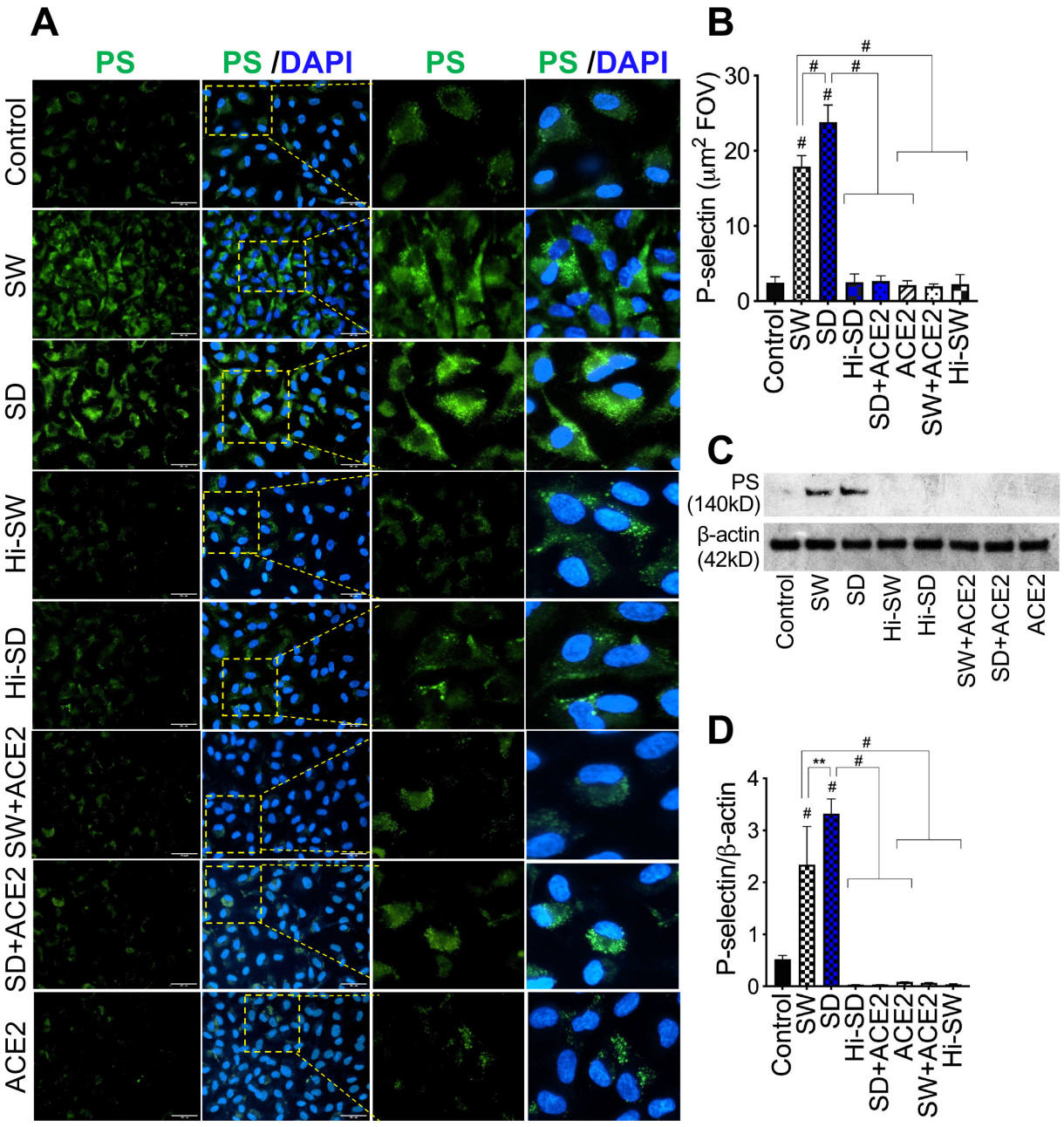

Figure 2. S-proteins induce P-selectin expression in HLMEC. HLMEC were treated with 1 nM S-proteins (SW or SD) for 12 h and P-selectin expression was quantified by immunofluorescence (**A**,**B**) and Western blot (**C**,**D**) analysis. DAPI (blue) was used for nuclear counterstaining. ImageJ software was used for densitometry quantification. For immunofluorescence images, five fields of view (FOV) were analyzed for each sample (**B**). For Western blot analysis, densitometry values were normalized to the sample's β-actin levels (**D**). For panel (**A**), all images were at 20×. PS: P-selectin; control: untreated cells; ACE2: cells treated with rhACE2; Hi: cells treated with heat-inactivated S-proteins ** $p = 0.01$; # $p < 0.0001$.

2.3. Delta Variant S-Proteins Induced Higher P-Selectin Transcription and Expression Than the Wuhan Variant

At 12 h, compared to SW, SD induced significantly higher P-selectin mRNA in HLMEC following direct exposure (3.7-fold, Figure 1A) or co-culture with neutrophils (2- to 6.8-fold, Figure 1B); and induced higher P-selectin mRNA in neutrophils (7.6- to 12.4-fold, Figure 1C). For neutrophils treated with S-proteins and co-cultured with HLMEC, SD induced 4-fold higher P-selectin transcription in HLMEC at 24 h (Figure 1D) and 2- to 15-fold higher P-selectin mRNA in neutrophils (Figure 1E), compared to SW. Immunofluorescence and Western blot analyses also showed that SD increased P-selectin expression in HLMEC by 1.3- to 1.4-fold compared to SW (Figure 2). No significant increase in P-selectin transcription (Figure 1) or expression (Figure 2) was observed in cells treated with Hi-SW or Hi-SD; recombinant human (rh) ACE2 blocked or significantly abrogated SW- and SD-induced P-selectin.

2.4. Exposure of Human Neutrophils and HLMEC to S-Proteins and Neutrophil–Endothelial Interactions Induces Histone H3 Citrullination

Hallmarks of NETosis include increased citrullination of histone proteins, including H3 [28–30]. Therefore, we assessed whether S-proteins and/or endothelial–neutrophil interactions affect the production of cit-H3. Compared to controls, SW and SD significantly increased cit-H3 levels in neutrophil culture supernatants following direct exposure (6–24 h) (1.6- to 3.3-fold, Figure 3A), co-culture of S-proteins-treated neutrophils with untreated HLMEC (2- to 4.3-fold, Figure 3B), or co-culture of S-proteins-treated endothelial cells with untreated neutrophils (1.7- to 3.3-fold, Figure 3C).

2.5. Exposure of HLMEC and Neutrophils to S-Proteins and Neutrophil–Endothelial Interactions Increased vWF Expression

Compared to controls, SW and SD significantly increased vWF levels in HLMEC culture supernatants (by 1.2- to 7.2-fold, Figure 4A) and cell lysates (2.2- to 5.2-fold, Figure 4B) following direct exposure (Figure 4A,B), co-culture of S-proteins-treated endothelial cells with untreated neutrophils (2- to 8.8-fold, Figure 4C), and co-culture of S-proteins-treated neutrophils with untreated HLMEC (1.5- to 4.6-fold, Figure 4D). Data showed a trend toward increased vWF following SD treatments and co-cultures, compared to SW (Figure 4).

2.6. Exposure of HLMEC and Neutrophils to S-Proteins and Endothelial-Neutrophil Interactions Increased IL-6 Expression

Compared to untreated cells, cells treated with Hi-SW, Hi-SD, or cells pretreated with rhACE2, exposure of HLMEC to SW or SD (6–24 h) increased IL-6 levels in culture supernatants by 1.2 to 4.6-fold (Figure 5A). Co-culture of SW- or SD-treated HLMEC with neutrophils increased IL-6 levels by 1.4 to 3.8-fold (Figure 5B). Compared to SW, SD induced significantly (1.3- to 1.6-fold) higher IL-6 expression following exposure to endothelial cells (Figure 5A) and co-culture of exposed endothelial cells with neutrophils (Figure 5B). Co-culture of SW- or SD-treated neutrophils with HLMEC increased IL-6 levels in culture supernatants by 1.4 to 4.7-fold (Figure 5C); rhACE2 blocked SW- and SD-induced IL-6. IL-6 levels in culture supernatants of cells treated with Hi-SW, Hi-SD, or rhACE2 were similar to untreated controls (Figure 5).

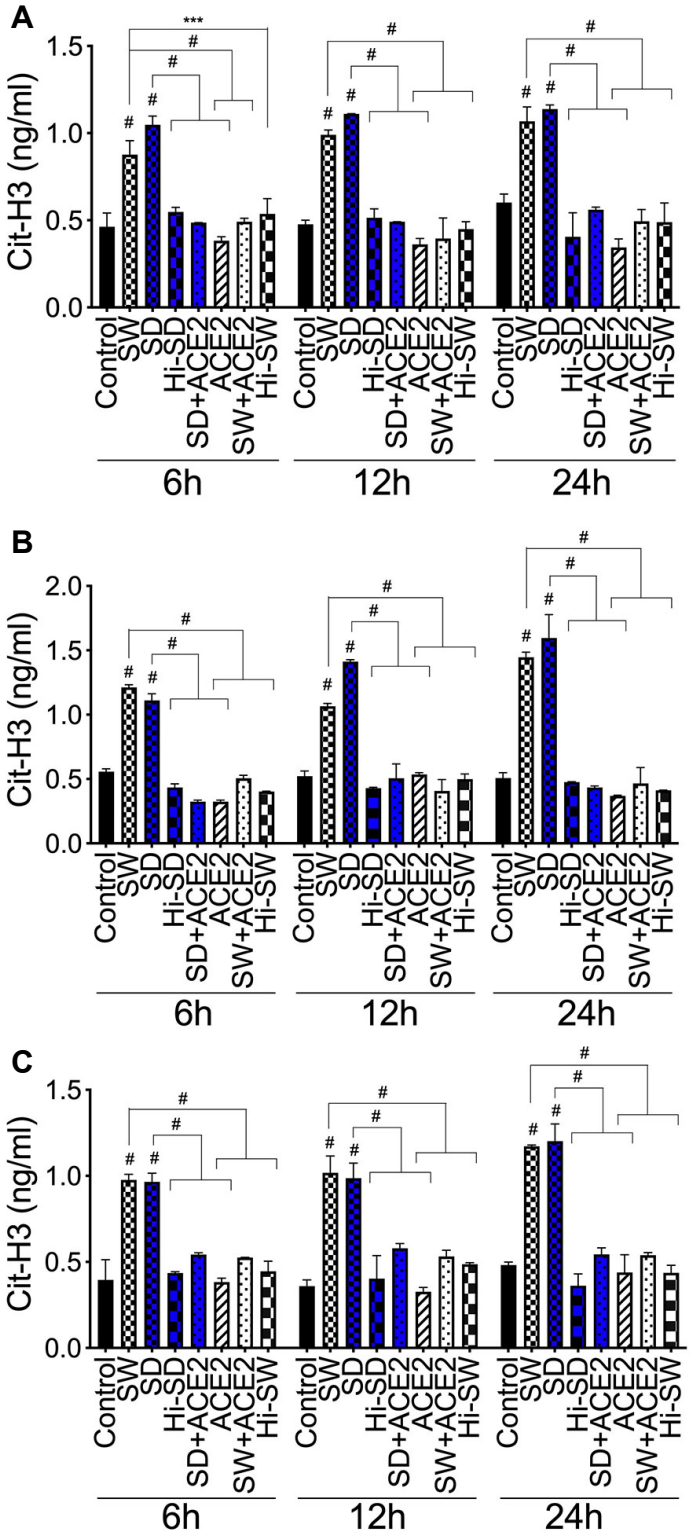

Figure 3. S-proteins and endothelial–neutrophil interactions induce/increase the expression and secretion of cit-H3. Human neutrophils were treated with 1 nM S-proteins (SW or SD) for 6–24 h (**A**). In separate experiments, neutrophils (**B**) and HLMEC (**C**) were treated with S-proteins for 6 h, washed, and co-cultured (for 6–24 h) with HLMEC (**B**) or neutrophils (**C**). Levels of cit-H3 in culture supernatants were quantified by ELISA. Data presented as mean ± standard deviation. Control: untreated cells; ACE2: cells treated with rhACE2; Hi: cells treated with heat-inactivated S-proteins. *** $p = 0.0003$; # $p < 0.0001$.

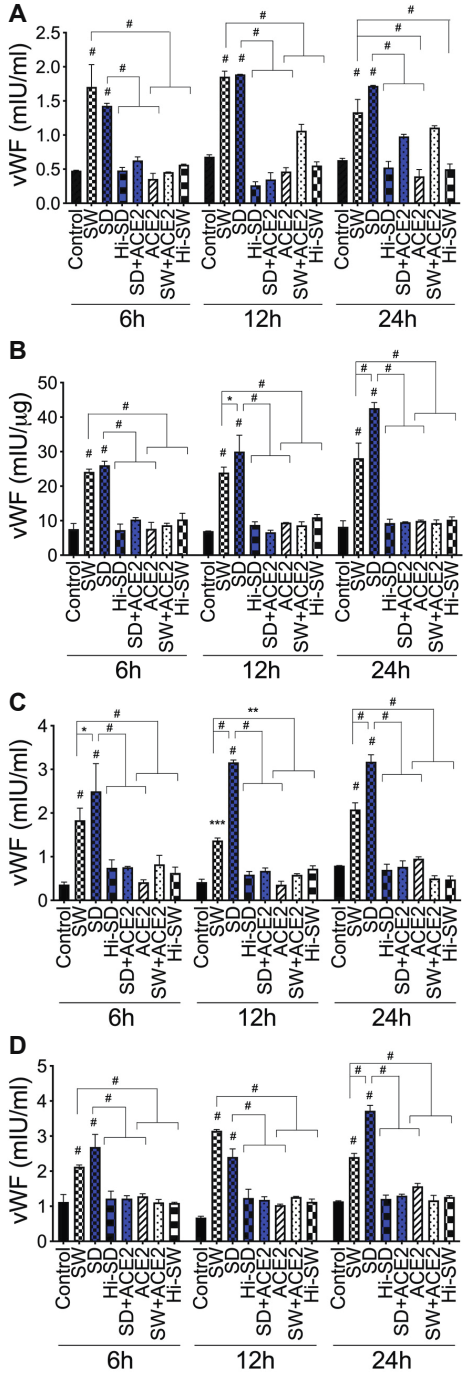

Figure 4. S-proteins and endothelial–neutrophil interactions induce vWF expression and release in HLMEC. (**A**,**B**) HLMEC were treated (for 6–24 h) with SW or SD (1 nM). HLMEC (**C**) and neutrophils (**D**) were treated (for 6 h) with SW or SD, washed, and co-cultured (for 6–24 h) with neutrophils (**C**) or endothelial cells (**D**). vWF levels in culture supernatants (**A**,**C**,**D**) and endothelial cell lysates (**B**) were quantified by ELISA. Data presented as mean ± standard deviation. Control: untreated cells; Hi: cells treated with heat-inactivated S-proteins; ACE2: cells treated with rhACE2. * $p < 0.03$; ** $p < 0.01$; *** $p = 0.0002$; # $p < 0.0001$.

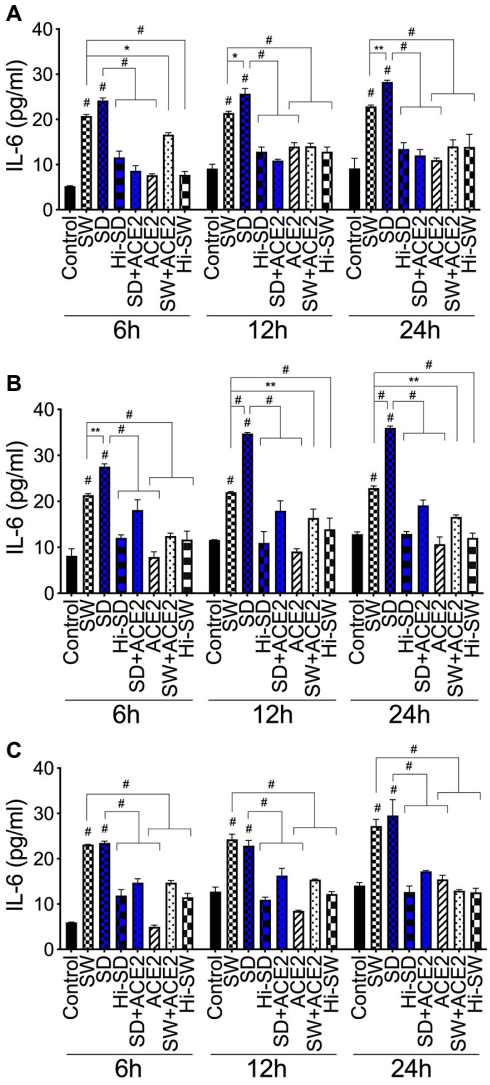

Figure 5. S-proteins and endothelial–neutrophil interactions increased IL-6 expression. (**A**) HLMEC treated (6–24 h) with SW or SD. HLMEC (**B**) and neutrophils (**C**) were treated (for 6 h) with SW or SD and co-cultured (for 6–24 h) with untreated neutrophils (**B**) or endothelial cells (**C**). IL-6 levels in culture supernatants were quantified by ELISA. Data presented as mean ± standard deviation. Control: untreated cells; ACE2: cells treated with rhACE2. Hi: cells treated with heat-inactivated S-proteins. * $p < 0.02$; ** $p < 0.005$; # $p < 0.0001$.

2.7. rTFPI Blocked S-Protein-Induced Citrullination of Histone H3, Expression and Secretion of vWF and IL-6

H3 citrullination: Compared to controls, exposure (24 h) of neutrophils to SW or SD increased cit-H3 levels in culture supernatants by 2.2- to 3.5-fold (Figure 6A); co-culture of SW- and SD-treated neutrophils with HLMEC increased cit-H3 levels by 2.3- to 3.5-fold (Figure 6B), and co-culture of SW- and SD-treated HLMEC with neutrophils increased cit-H3 levels by 2.8- to 3.7-fold (Figure 6C). rTFPI blocked SW- and SD-induced H3 citrullination. Pretreatment with rTFPI reduced SW- and SD-induced H3 citrullination in neutrophils (by 3-fold, Figure 5A); reduced H3 citrullination induced by co-culture of SW- and SD-treated neutrophils with HLMEC (by 3.2- to 3.7-fold; Figure 6B); and reduced H3 citrullination induced by co-culture of SW- and SD-treated HLMEC with neutrophils (by 3.2- to 3.6-fold; Figure 6C).

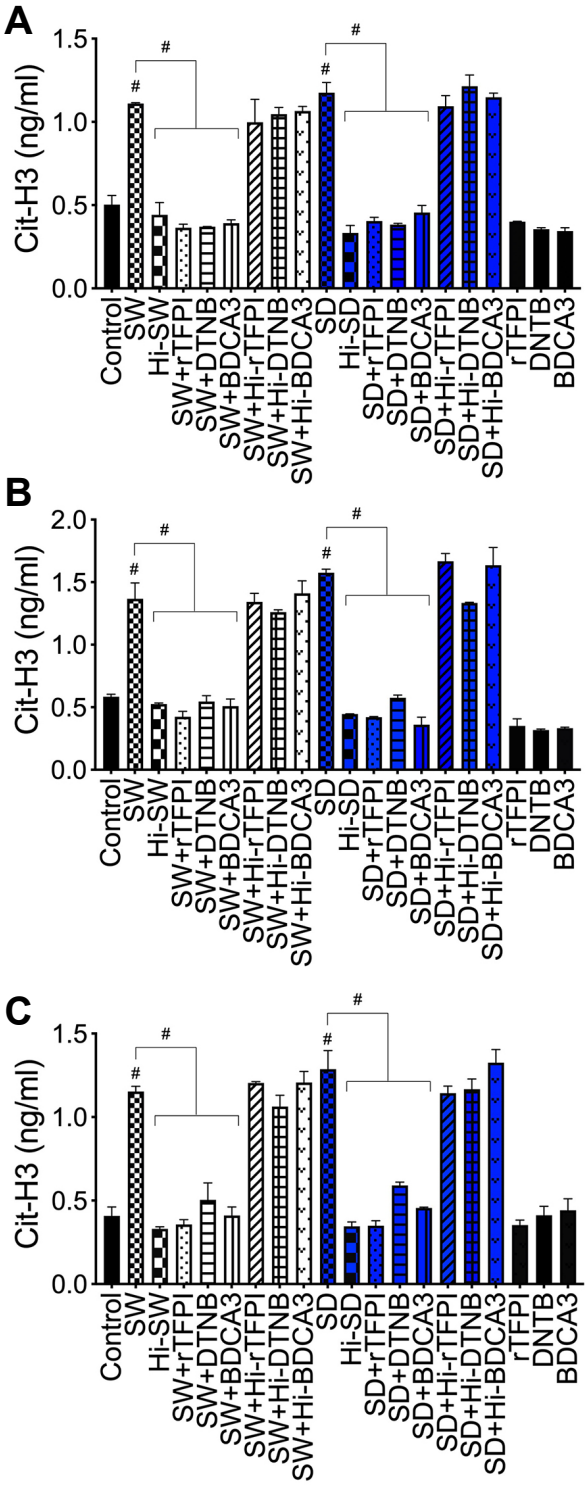

Figure 6. rTFPI, thrombomodulin (BDCA3), and thiol blockers (DTNB) prevent S-protein-induced H3 citrullination. (**A**): human neutrophils treated for 24 h with SW or SD, with or without rTFPI, DTNB, and BDCA3 (200 ng/mL). Neutrophils (**B**) and HLMEC (**C**) were treated (6 h) with SW or SD, with or without rTFPI, DTNB, and BDCA3, washed, and co-cultured (for 24 h) with HLMEC (**B**) or neutrophils (**C**). cit-H3 levels in culture supernatants quantified by ELISA. Data presented as mean ± standard deviation. Control: untreated cells; Hi: heat-inactivated (SW, SD, rTFPI, DTNB, BDCA3). # $p < 0.0001$.

vWF: Compared to controls, 24 h exposure of HLMEC to SW or SD increased vWF levels in culture supernatants (by 6.3- to 9.4-fold; Figure 7A) and cell lysates (by 8.7 to 14.6-fold; Figure 7B). Co-culture of SW- and SD-treated HLMEC with neutrophils increased vWF in culture supernatants by 6.5- to 9.8-fold (Figure 7C), and co-culture of SW- and SD-treated neutrophils with HLMEC increased vWF in culture supernatants by 5.8- to 8.7-fold (Figure 7D). rTFPI blocked SW- and SD-induced vWF expression and secretion. Pretreatment with rTFPI reduced SW- and SD-induced vWF in HLMEC culture supernatants (by 4.7- to 8-fold, Figure 7A) and cell lysates (by 11.4- to 17-fold, Figure 7B); reduced vWF induced by co-culture of SW- and SD-treated HLMEC with neutrophils (by 7.4-fold; Figure 7C); and reduced vWF induced by co-culture of SW- and SD-treated neutrophils with endothelial cells (by 6.3- to 8.5-fold; Figure 7D).

IL-6: Compared to controls, 24 h exposure of HLMEC to SW or SD increased IL-6 levels in culture supernatants by 1.8- to 2.6-fold (Figure 8A). Co-culture of SW- and SD-treated HLMEC with untreated neutrophils increased IL-6 expression by 2-fold (Figure 8B), and co-culture of SW- and SD-treated neutrophils with untreated HLMEC increased IL-6 expression by 1.8- to 2-fold (Figure 8C). rTFPI blocked SW- and SD-induced IL-6 expression. Pretreatment with rTFPI reduced SW- and SD-induced IL-6 in HLMEC culture supernatants (by 1.6 to 1.9-fold, Figure 8A); reduced IL-6 induced by co-culture of SW- and SD-treated HLMEC with neutrophils (by 2-fold; Figure 8B); and reduced IL-6 induced by co-culture of SW- and SD-treated neutrophils with endothelial cells (by 1.8-fold; Figure 8C).

2.8. DTNB Blocked S-Protein-Induced Citrullination of Histone H3, Expression and Secretion of vWF and IL-6

H3 citrullination. DTNB blocked SW- and SD-induced H3 citrullination. Pretreatment with DTNB reduced SW- and SD-induced H3 citrullination in neutrophils (by 3-fold, Figure 6A); reduced H3 citrullination induced by co-culture of SW- and SD-treated neutrophils with HLMEC (by 2.5- to 2.7-fold; Figure 6B); and reduced H3 citrullination induced by co-culture of SW- and SD-treated HLMEC with neutrophils (by 2.2- to 2.3-fold, Figure 6C).

vWF. DTNB blocked SW- and SD-induced vWF expression: reduced SW- and SD-induced vWF in HLMEC culture supernatants (by 6.5- to 9-fold, Figure 6A) and cell lysates (by 10- to 13-fold, Figure 7B); reduced vWF induced by co-culture of SW- and SD-treated HLMEC with neutrophils (by 8- to 10-fold; Figure 7C); and reduced vWF induced by co-culture of SW- and SD-treated neutrophils with EC (by 5- to 8-fold; Figure 7D).

IL-6. DTNB blocked SW- and SD-induced IL-6 expression and secretion: reduced SW- and SD-induced IL-6 in HLMEC culture supernatants (by 1.6- to 1.9-fold, Figure 8A); reduced IL-6 induced by co-culture of SW- and SD-treated HLMEC with neutrophils (by 2-fold; Figure 8B); and reduced IL-6 induced by co-culture of SW- and SD-treated neutrophils with HLMEC (by 1.7- 1.8-fold; Figure 8C).

2.9. Thrombomodulin Blocked S-Protein-Induced Citrullination of Histone H3 and Blocked vWF and IL-6 Expression and Secretion

H3 citrullination. Thrombomodulin (TM, BDCA3) blocked SW- and SD-induced H3 citrullination. Pretreatment with TM reduced SW- and SD-induced H3 citrullination in neutrophils (by 2.6- to 2.8-fold, Figure 6A); reduced H3 citrullination induced by co-culture of SW- and SD-treated neutrophils with HLMEC (by 2.7- to 4.4-fold; Figure 6B); and reduced H3 citrullination induced by co-culture of SW- and SD-treated HLMEC with neutrophils (by 2.8-fold; Figure 6C).

vWF. TM blocked SW- and SD-induced vWF expression: reduced SW- and SD-induced vWF in HLMEC culture supernatants (by 4- to 13-fold, Figure 6A) and cell lysates (by 9- to 17-fold, Figure 7B); reduced vWF induced by co-culture of SW- and SD-treated HLMEC with neutrophils (by 7- to 8-fold; Figure 7C); and reduced vWF induced by co-culture of SW- and SD-treated neutrophils with endothelial cells (by 6.2- to 10.2-fold; Figure 7D).

IL-6. TM blocked SW- and SD-induced IL-6 expression: reduced SW- and SD-induced IL-6 in HLMEC culture supernatants (by 1.6- to 2.3-fold, Figure 8A); reduced IL-6 induced

by co-culture of SW- and SD-treated HLMEC with neutrophils (by 2-fold; Figure 8B); and reduced IL-6 induced by co-culture of SW- and SD-treated neutrophils with EC (by 1.7- to 1.9-fold; Figure 8C).

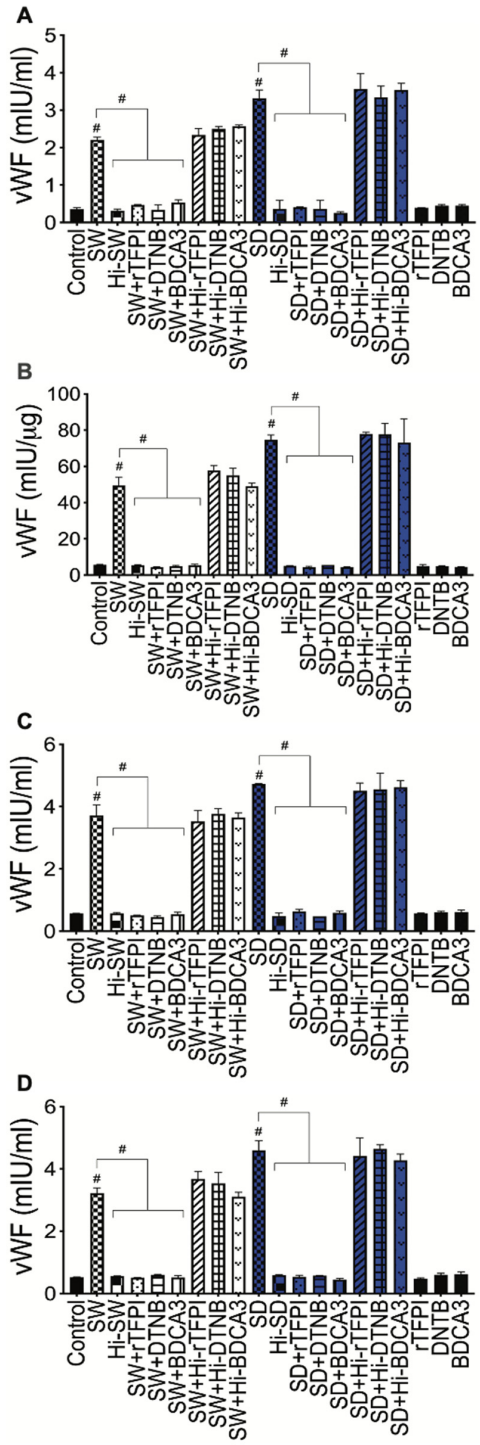

Figure 7. rTFPI, thrombomodulin, and thiol blockers prevent S-protein-induced vWF expression. (**A**,**B**) HLMEC were treated (24 h) with SW or SD, with or without rTFPI, DTNB, and BDCA3. HLMEC (**C**) and neutrophils (**D**) were treated (6 h) with SW or SD, with or without rTFPI, DTNB, and BDCA3, washed, and co-cultured (for 24 h) with neutrophils (**C**) or HLMEC (**D**). vWF levels in culture supernatants (**A**,**C**,**D**) and endothelial cell lysates (**B**) were quantified by ELISA. Data presented as mean ± standard deviation. Control: untreated cells; Hi: heat-inactivated (SW, SD, rTFPI, DTNB, BDCA3). # $p < 0.0001$.

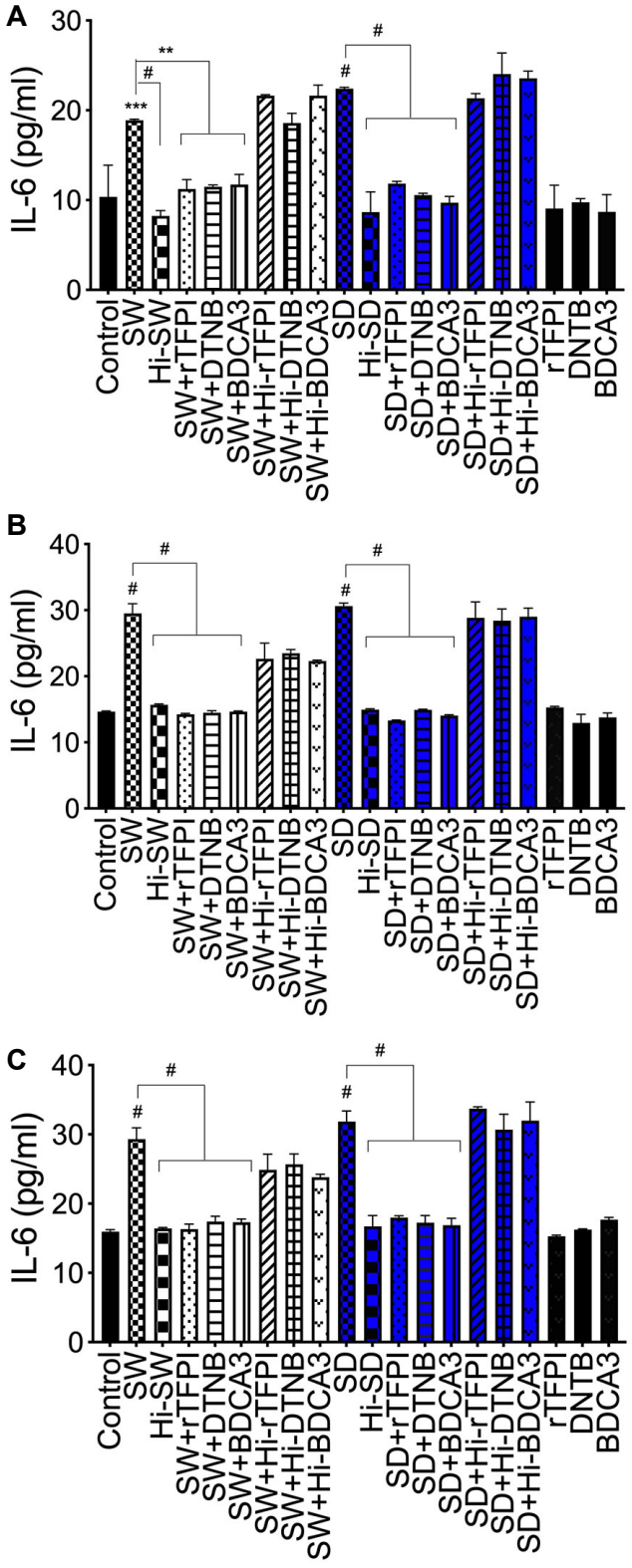

Figure 8. rTFPI, thrombomodulin, and thiol blockers prevent S-protein-induced IL-6 expression. (**A**) HLMEC were treated (24 h) with SW or SD, with or without rTFPI, DTNB, and BDCA3. HLMEC (**B**) and neutrophils (**C**) were treated (6 h) with SW or SD, with or without rTFPI, DTNB, and BDCA3, washed, and co-cultured (for 24 h) with neutrophils (**B**) or HLMEC (**C**). IL-6 levels in culture supernatants were quantified by ELISA. Data presented as mean ± standard deviation. Control: untreated cells; Hi: heat-inactivated (SW, SD, rTFPI, DTNB, BDCA3). ** $p < 0.007$; *** $p = 0.0009$; # $p < 0.0001$.

3. Discussion

The lungs are a prime target for SARS-CoV-2 infection. COVID-19 disease progression is often associated with acute respiratory distress syndrome involving severe lung injury, increased inflammation and coagulopathy [4,5,31,32], as well as increased leukocyte infiltration into tissues associated with endothelial apoptosis and microcirculatory clots [4–6]. The pathogenesis of these pulmonary complications in COVID-19 patients is unknown. Considering that neutrophils are the most abundant leukocytes in humans [33], that blood leukocytes infiltrate tissues by transmigrating through the vascular endothelium, and that S-proteins can be shed and are present in bodily fluids, microvessels, and tissues of SARS-CoV-2 infected patients [7,17], we investigated the effect of S-proteins and endothelial–neutrophils interactions on the adhesion molecule P-selectin, markers of endothelial injury and increased coagulopathy (vWF), NETosis (cit-H3) and inflammation (IL-6).

We demonstrate that exposure of HLMEC or neutrophils to S-proteins and endothelial–neutrophils interactions significantly increased IL-6 expression and secretion. S-proteins have also been shown to increase the production of IL-6 and other inflammatory cytokines and chemokines in endothelial cells from other vascular beds, including human aortic endothelial cells [34], as well as in human pulmonary epithelial cells [35,36], peripheral blood mononuclear cells and human and murine macrophages [37–39]. Studies of COVID-19 patients also showed significant increases in proinflammatory cytokines and chemokines, including IL-6, IL-1β, TNF-α, and granulocyte–macrophage colony-stimulating factor, in patients' plasma, with much higher levels in the plasma of critically ill patients [40]. Our current study suggests that following SARS-CoV-2 infection, viral S-proteins contribute to inflammation of the lung endothelium and disease pathology; and that in the presence of S-proteins, endothelial–neutrophil interactions also induce inflammation.

P-selectin is expressed on activated endothelial cells, platelets and leukocytes, and functions as an adhesion molecule. During inflammatory responses, P-selectin plays a critical role in the recruitment and aggregation of platelets and leukocytes to the vascular wall and to areas of vascular and tissue injury [41,42]. Our data show that S-proteins increase P-selectin transcription and expression in HLMEC, and co-culture of S-protein-treated endothelial cells with non-treated neutrophils or co-culture of S-protein-treated neutrophils with non-treated endothelial cells further increases P-selectin in both HLMEC and neutrophils. These results suggest that S-protein-induced P-selectin would increase leukocyte adhesion to the lung endothelium and infiltration into lung tissues and that endothelial–neutrophil interactions further potentiate leukocyte adhesion and transmigration into tissues.

Our data also showed that exposure of HLMEC to S-proteins increased vWF expression and release, and co-culture of S-protein-treated endothelial cells with non-treated neutrophils, or co-culture of S-protein-treated neutrophils with non-treated endothelial cells, further increased vWF expression and secretion. vWF are stored in endothelial granules (Weibel–Palade bodies) and are released/secreted following endothelial activation [43]; vWF released further mediates the adhesion of platelets and leukocytes to the vascular endothelium and their recruitment to sites of injury. Thus, increased vWF release is a marker of endothelial activation and vascular injury [44]. vWF is a carrier of factor (F)-VIII and both vWF and F-VIII increase fibrin generation and coagulopathy [45]. Our previous study showed that exposure of human endothelial cells or neutrophils to S-proteins and endothelial–neutrophils interactions, increased expression and release of prothrombogenic factors, including tissue factor (TF), fibrinogen, and thrombin, via the TF pathway [46]. Our current findings are in agreement with clinical data showing that COVID-19 patients have significantly increased levels of circulating P-selectin, vWF antigen, and F-VIII activity [6,47–49]. The highest levels of P-selectin, vWF antigen, and F-VIII activity were observed among critically ill patients and were associated with thrombosis, severe disease, lower rates of hospital discharge, and higher mortality [6,47–49].

Our current study also demonstrates that exposure of neutrophils to S-proteins and neutrophil–endothelial interactions significantly increased the formation and release of cit-H3. Histone citrullination is a hallmark of NETosis and is mediated by peptidyl arginine deiminase-4 following neutrophil activation [28,50–52]. This citrullination leads to a loss of charge and deamination of histone arginine residues, which alter histone DNA and protein-binding properties and enable chromatin decondensation and the release of nuclear DNA fragments [50–52]. Thus, when activated, neutrophils can release NETs, which consist of web-like structures composed of double-stranded (ds) DNA, citrullinated histones and granule proteins [28,50–52]. NETosis has been linked to coagulopathy and thrombosis. NET components have been shown to degrade TFPI, thus activating the coagulation cascade TF pathway [53]. NETs released can further serve as a scaffold for the binding of other procoagulant molecules such as vWF, fibronectin, and fibrinogen [54], thus trapping circulating blood cells and promoting their aggregation, resulting in the formation of thrombi and vessel occlusion [54,55]. NET components (histones, dsDNA) further promote thrombosis by increasing the thickness, rigidity, and stability of fibrin fibers and impeding fibrinolysis [56,57].

Our current data showing that exposure of human neutrophils to S-proteins and neutrophil–endothelial interaction increases the production and release of a NET component (cit-H3) are in agreement with clinical studies showing increased NETosis in COVID-19. Plasma, neutrophils, and lung fluids from COVID-19 patients showed increased markers of neutrophil activation and NET components, including cit-H3, myeloperoxidase (MPO), and the MPO-DNA complex [19,40]. Exposure of healthy human neutrophils to SARS-CoV-2 virions also induced the release of NET components, including the MPO, MPO-DNA complex, and cit-H3 [19]. The NETs produced can further injure the vascular endothelium. There is evidence that NETs can induce toxicity, apoptosis, and dysfunction of the vascular endothelium; induce endothelial cell expression and release of adhesion molecules and TF, thus further promoting leukocyte recruitment to the vascular endothelium and thrombosis [53,58–60]. NETs produced following SARS-CoV-2 treatment of neutrophils also induced apoptosis in lung epithelial cells [19].

Our current data showed that compared to SW, exposure of HLMEC or neutrophils to SD and endothelial–neutrophil interactions induced 2- to 15-fold higher P-selectin transcription and significantly higher expression of P-selectin, IL-6 and vWF. Our previous studies also demonstrated that, compared to SW, exposure of HLMEC or neutrophils to SD and endothelial–neutrophil interactions induced significantly higher TF levels [46]. This evidence suggests that different SARS-CoV-2 genetic variants and subvariants that have been driving waves of infection and disease epidemiology since the beginning of the COVID-19 pandemic [61–63], can influence the production of pro-thrombotic factors, inflammation, leukocyte adhesion to the vascular endothelium and infiltration into tissues. These differential effects of SARS-CoV-2 variants and genotypes would influence disease pathology in infected individuals.

We previously demonstrated that exposure of HLMEC or neutrophils to S-proteins and neutrophil–endothelial interactions induced prothrombogenic factors (TF, F-V, thrombin, and fibrinogen), inhibited TFPI, and that both rTFPI and DTNB blocked S-protein-induced upregulation of F-V, thrombin, and fibrinogen [46]. TFPI is a serine protease inhibitor that inhibits TF activity and blocks the coagulation cascade extrinsic pathway [64–66]. Disulfide bonds are essential for TF activation and increased TF activity that drives the coagulation extrinsic pathway signaling cascade [67–69]. DTNB reacts with free thiol groups to prevent the formation of disulfide bonds [70], and thiol-based drugs can decrease S-proteins binding to ACE2, inhibit viral entry and infection, and decrease SARS-CoV-2-induced inflammation of lung neutrophils [71,72]. Our current data show that rTFPI and DTNB also blocked S-protein-induced expression and secretion of IL-6, vWF, and cit-H3. These results suggest that following direct contact of SARS-CoV-2 with the pulmonary endothelium or neutrophils, and endothelial–neutrophil interactions, viral S-proteins induce endothe-

lial degranulation (leading to the release of vWF from cellular granules), NETosis and inflammation via the TF pathway and mechanisms involving functional thiol groups.

TM is an endothelial receptor and a natural anticoagulant that binds thrombin to form a stable thrombin–TM complex that induces fibrinolysis and prevent/reduce coagulation [27]. We previously demonstrated that TM blocked S-protein-induced upregulation of fibrinogen but had no effect on S-protein-induced expression of F-V or thrombin [46]. Our current study demonstrates that TM blocks S-protein-induced increases in IL-6, vWF, and cit-H3 production. These results suggest that SARS-CoV-2-induced vWF, NETosis, and inflammation occur downstream of the coagulation TF pathway, and as TM binds thrombin and limits the intrinsic and common pathways of the coagulation cascade, it abrogates vWF production, inflammation and NETosis.

Because S-proteins are shed by infected cells in vivo and most COVID-19 vaccines encode SARS-CoV-2 S-proteins, increases in markers of inflammation, coagulopathy, and NETosis following exposure of neutrophils and lung endothelial cells to S-proteins could explain some vascular complications observed in COVID-19 patients [73] and post-COVID-19 vaccination adverse events. In fact, reported post vaccination complications include increased vasculitis, endothelial activation, increased inflammatory cytokines and chemokines, and thrombosis [74–76]. Studies in a SARS-CoV-2 mouse model showed that the S-protein S1 subunit was primarily responsible for the observed lung injury, increase in inflammatory cytokines and blood cells in lung fluids [77]. In vitro studies also showed that S1 significantly decreased trans-endothelial electric resistance and increased endothelial permeability [77]. Our future studies will determine whether a specific S-protein subunit is responsible for the increased coagulopathy, histone citrullination and inflammation observed in our current study.

In summary, our current data demonstrate that exposure of primary HLMEC or neutrophils to S-proteins and endothelial–neutrophil interactions increased the transcription and expression of P-selectin (adhesion molecule), increased the expression and secretion of markers of endothelial activation and coagulopathy (vWF), NETosis (cit-H3) and inflammation (IL-6). rTFPI, DNTB, and TM prevented these S-protein-induced effects (Figure 9), which suggests that following SARS-CoV-2 contact with the lung endothelium or neutrophils and endothelial–neutrophil interactions, viral S-proteins induce inflammation, NETosis, and coagulopathy via the TF pathway and mechanisms involving free and functional thiol groups. These findings also suggest that therapeutic strategies against SARS-CoV-2-induced inflammation, NETosis, and coagulopathy could include supplementation with rTFPI, natural anticoagulants such as TM, and/or thiol-based drugs.

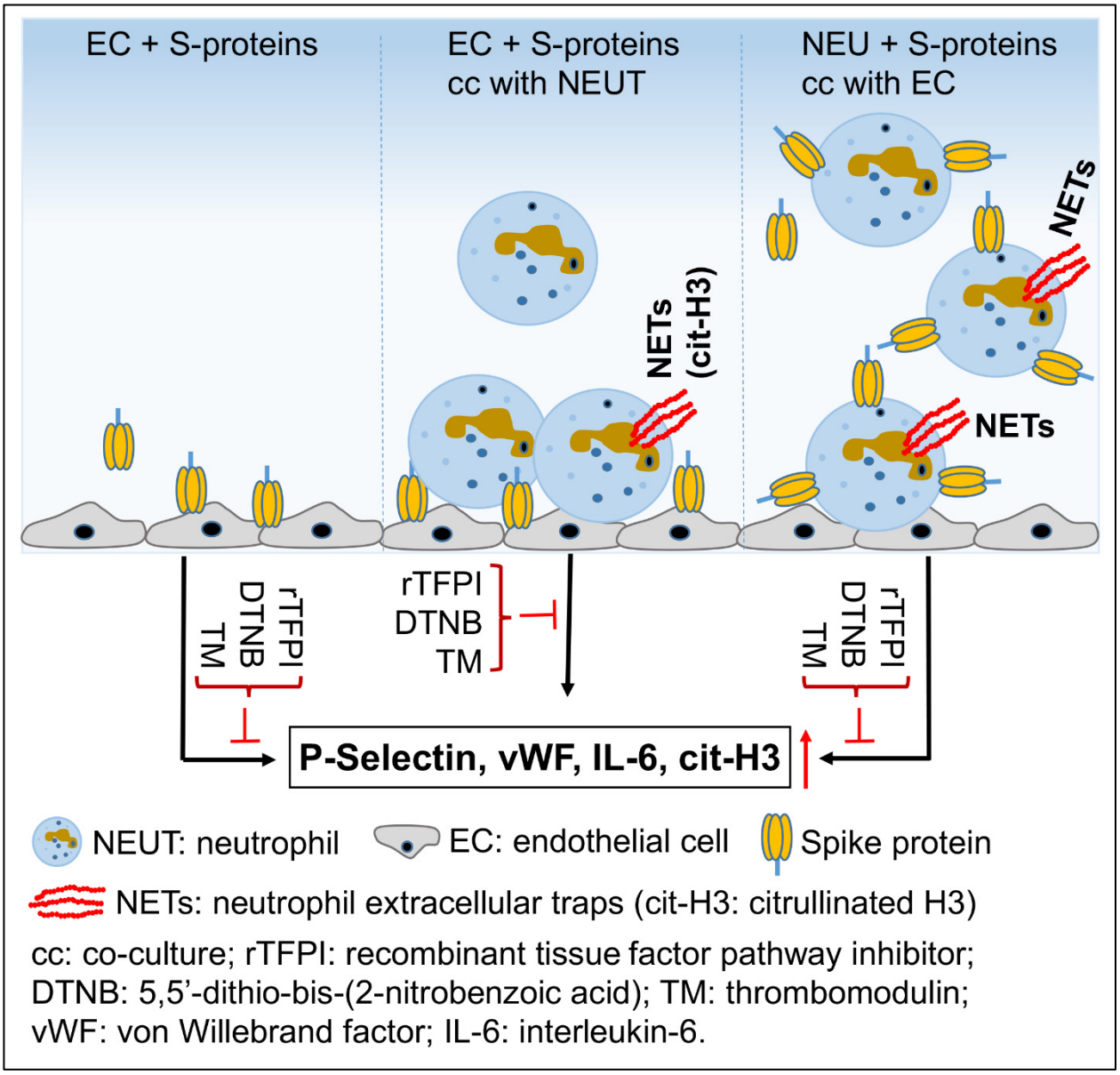

Figure 9. Model illustrating S-protein-induced P-selectin, vWF, IL-6 and cit-H3. Arrows indicate direct activation. The red arrows indicate upregulation; the red perpendicular symbol (⊥) indicates pharmacological inhibitors.

4. Materials and Methods

4.1. Reagents

Recombinant SARS-CoV-2 S-proteins, SW, SD, rhACE2, rTFPI, and TM (BDCA3), were purchased from R&D Systems (Minneapolis, MN, USA). DTNB was from Sigma-Aldrich (St. Louis, MO, USA). Anti-human CD66b and anti-human CD45 antibodies were from Stemcell Technologies (Cambridge, MA, USA); anti-human CD16 antibodies were from Ancell Corporation (Stillwater, MN, USA). Monoclonal P-selectin antibodies and DAPI were from Thermo Fisher/Invitrogen (Waltham, MA, USA), and β-actin antibodies were from Santa Cruz Biotechnology (Dallas, TX, USA).

4.2. HLMEC and Neutrophils

Primary HLMEC was obtained from Lonza (Houston, TX, USA), cultured to confluence as previously described [78–80], and used at passages 2 to 4. Blood samples were obtained from human donors seronegative for HIV-1, HIV-2, and hepatitis-B [80,81]. Neu-

trophils were isolated from fresh donor blood using the EasySep direct human neutrophil isolation kit (Stemcell Technologies), and their purity was confirmed by FACS as previously described using antibodies to human CD16, CD66b, and CD45 [46].

4.3. Cell Treatment and Endothelial–Neutrophil Co-Culture

S-proteins (both SW and SD) were used at 1 nM and rTFPI, DTNB, and BDCA3 at 200 ng/mL, based on previous studies showing that these doses do not decrease cellular viability [46,82]. Treatment of HLMEC and neutrophils with SW and SD, pre-treatment with rTFPI, DTNB, and BDCA3, culture, co-culture, collection of culture supernatants and harvesting of neutrophils and endothelial cells were performed as previously described [46]. Controls included untreated cells, cells treated with heat-inactivated (Hi) S-proteins, rTFPI, DTNB, or BDCA3, and cells pretreated with rhACE2 (1 μg/mL) to block S-protein binding.

4.4. RNA Isolation and Real-Time PCR

Total RNA was extracted from cells using the Trizol reagent (Life Technologies-Ambion, Austin, TX, USA), RNA quality was checked, and reverse transcription was performed using the Verso cDNA synthesis kit (ThermoFisher) as previously described [46]. Real-time PCR was performed using the LightCycler 480 II (Roche, Basel, Switzerland) Real-Time PCR System. Experimental details and cycling conditions were as previously described, using the following Applied Biosystems (Waltham, MA, USA) primers: Selectin-P (Hs00927900_m1) and GAPDH (Hs02786624_g1). P-selectin mRNA levels were quantified using the Delta-CT method and normalized to the sample's GAPDH levels.

4.5. Human vWF, cit-H3, and IL-6 ELISA

Following treatments, culture supernatants and cells were collected; cells were lysed in mammalian cell lysis buffer (CelLytic M, Sigma) and their protein content quantified using the bicinchoninic acid assay, as previously described [83–85]. Levels of vWF, cit-H3, and IL-6 in each culture supernatant (100 μL), as well as vWF levels in cell lysates (100 μL containing 50 μg protein), were quantified by ELISA using human vWF (Abcam, Waltham, MA, USA), cit-H3 (Cayman Chemical, Ann Arbor, MI, USA), and IL-6 (Invitrogen) ELISA kits in accordance with the manufacturer's protocols. Standard curves from human vWF, cit-H3, and IL-6 reference standards (provided with each kit) were used, respectively, to quantify vWF, cit-H3, and IL-6 levels in each sample. Data were analyzed using Student's *t*-test (two-tailed) or analysis of variance, followed by Tukey's multiple-comparison tests, as previously described [46].For all figures, data are presented as mean ± standard deviation.

4.6. Immunofluorescence Analysis

Primary HLMEC were cultured to confluence on collagen-coated coverslips, treated for 12 h with S-proteins and analyzed by immunofluorescence as previously described [85] using antibodies to P-selectin (Thermo Fisher Scientific, Waltham, MA, USA) diluted 1:100 in PBS containing 0.1% Tween 20 and 1% bovine serum albumin (PBST); and fluorescein isothiocyanate-conjugated secondary antibodies (1:2000 in PBST). Coverslips were mounted using Prolong™ Gold anti-fade mounting medium with DAPI (Invitrogen) and sealed as we previously described. Images were captured using an Eclipse TE20000-U fluorescent microscope (Nikon, Melville, NY, USA) and an Infinity 3–6 urfm monochrome camera (Luminera, Lod, Israel). Semi-quantitative analysis of P-selectin expression was performed using computer-assisted image analysis of the ImageJ software, and five fields of view (FOV) were analyzed for each sample. The staining intensity was normalized to surface area (μm^2) and averaged to estimate protein expression (μm^2 FOV).

4.7. Western Blot Analysis

Primary HLMEC cultured to confluence in six-well plates were treated for 12 h with S-proteins, harvested and lysed in CelLytic™ M buffer (Sigma) containing protease inhibitors. The total protein concentration in each sample was quantified using the Bicin-

choninic Acid assay as previously described [83,85,86]. Protein samples (30 μg each) were analyzed by sodium dodecyl sulfate-polyacrylamide gel electrophoresis as previously described [83,85,86] using monoclonal antibodies to P-selectin and β-actin (each at 1:1000 dilution). Densitometry analysis was performed using the ImageJ (V.1.54f 29) software; each sample's P-selectin level was normalized to its β-actin levels.

Author Contributions: Conceptualization, G.D.K.; investigation, B.B. and G.D.K.; data curation, B.B. and G.D.K.; formal analysis, B.B. and G.D.K.; writing—original draft, review, revision and editing, G.D.K. All authors have read and agreed to the published version of the manuscript.

Funding: This work was supported by a Faculty Diversity Award from UNMC.

Institutional Review Board Statement: Not applicable.

Informed Consent Statement: Not applicable.

Data Availability Statement: All data generated or analyzed during this study are included in this publication and/or are available from the corresponding author on reasonable request.

Acknowledgments: We thank the UNMC Elutriation Core Facility for assistance with obtaining donors' blood for neutrophils isolation.

Conflicts of Interest: The authors declare no conflict of interest.

Abbreviations

DTNB	5:5′-dithio-bis-(2-nitrobenzoic acid)
TFPI	Tissue factor pathway inhibitor
rTFPI	Recombinant tissue factor pathway inhibitor
BDCA3/TM	Thrombomodulin
vWF	von Willebrand factor
IL-6	Interleukin-6
Cit-H3	Citrulinated histone 3
dsDNA	Double strand DNA
NETs	Neutrophils extracellular traps
MPO	Myeloperoxidase
TF	Tissue factor
F-V	Factor-V
F-VIII	Factor-VIII
SARS-CoV-2	Severe acute respiratory syndrome coronavirus-2
COVID-19	Coronavirus disease 2019
ACE2	Angiotensin-converting enzyme-2
rhACE2	Recombinant human ACE2
S-proteins	Spike proteins
SW	Spike protein: Wuhan variant
SD	Spike protein: delta variant
Hi	Heat-inactivated
ELISA	Enzyme-linked immunosorbent assay
PCR	Polymerase chain reaction
cDNA	Complementary DNA
GAPDH	Glyceraldehyde-3-Phosphate Dehydrogenase

References

1. JHU. Coronavirus Resource Center: COVID-19 in the USA. 2023. Available online: https://coronavirus.jhu.edu/ (accessed on 24 April 2023).
2. CDC. *United States COVID-19 Cases and Deaths by State*; US Center for Disease Control and Prevention: Atlanta, GA, USA, 2023. Available online: https://www.cdc.gov/covid-data-tracker/#cases (accessed on 24 April 2023).
3. WHO. *Coronavirus Disease (COVID-19) Pandemic*; World Health Organization: Geneva, Switzerland, 2023; Available online: https://www.who.int/emergencies/diseases/novel-coronavirus-2019 (accessed on 24 April 2023).

4. Ackermann, M.; Verleden, S.E.; Kuehnel, M.; Haverich, A.; Welte, T.; Laenger, F.; Vanstapel, A.; Werlein, C.; Stark, H.; Tzankov, A.; et al. Pulmonary Vascular Endothelialitis, Thrombosis, and Angiogenesis in COVID-19. *N. Engl. J. Med.* **2020**, *383*, 120–128. [CrossRef]
5. Varga, Z.; Flammer, A.J.; Steiger, P.; Haberecker, M.; Andermatt, R.; Zinkernagel, A.S.; Mehra, M.R.; Schuepbach, R.A.; Ruschitzka, F.; Moch, H. Endothelial cell infection and endotheliitis in COVID-19. *Lancet* **2020**, *395*, 1417–1418. [CrossRef]
6. O'Sullivan, J.M.; Gonagle, D.M.; Ward, S.E.; Preston, R.J.S.; O'Donnell, J.S. Endothelial cells orchestrate COVID-19 coagulopathy. *Lancet Haematol.* **2020**, *7*, e553–e555. [CrossRef] [PubMed]
7. Magro, C.; Mulvey, J.J.; Berlin, D.; Nuovo, G.; Salvatore, S.; Harp, J.; Baxter-Stoltzfus, A.; Laurence, J. Complement associated microvascular injury and thrombosis in the pathogenesis of severe COVID-19 infection: A report of five cases. *Transl. Res.* **2020**, *220*, 1–13. [CrossRef] [PubMed]
8. Villanueva, E.; Yalavarthi, S.; Berthier, C.C.; Hodgin, J.B.; Khandpur, R.; Lin, A.M.; Rubin, C.J.; Zhao, W.; Olsen, S.H.; Klinker, M.; et al. Netting neutrophils induce endothelial damage, infiltrate tissues, and expose immunostimulatory molecules in systemic lupus erythematosus. *J. Immunol.* **2011**, *187*, 538–552. [CrossRef] [PubMed]
9. Schnoor, M.; Alcaide, P.; Voisin, M.B.; van Buul, J.D. Crossing the Vascular Wall: Common and Unique Mechanisms Exploited by Different Leukocyte Subsets during Extravasation. *Mediat. Inflamm.* **2015**, *2015*, 946509. [CrossRef]
10. Yan, R.; Zhang, Y.; Li, Y.; Xia, L.; Guo, Y.; Zhou, Q. Structural basis for the recognition of SARS-CoV-2 by full-length human ACE2. *Science* **2020**, *367*, 1444–1448. [CrossRef] [PubMed]
11. Chan, K.K.; Dorosky, D.; Sharma, P.; Abbasi, S.A.; Dye, J.M.; Kranz, D.M.; Herbert, A.S.; Procko, E. Engineering human ACE2 to optimize binding to the spike protein of SARS coronavirus 2. *Science* **2020**, *369*, 1261–1265. [CrossRef] [PubMed]
12. McKenna, E.; Wubben, R.; Isaza-Correa, J.M.; Melo, A.M.; Mhaonaigh, A.U.; Conlon, N.; O'Donnell, J.S.; Ni Cheallaigh, C.; Hurley, T.; Stevenson, N.J.; et al. Neutrophils in COVID-19: Not Innocent Bystanders. *Front. Immunol.* **2022**, *13*, 864387. [CrossRef]
13. Calvert, B.A.; Quiroz, E.J.; Lorenzana, Z.; Doan, N.; Kim, S.; Senger, C.N.; Anders, J.J.; Wallace, W.D.; Salomon, M.P.; Henley, J.; et al. Neutrophilic inflammation promotes SARS-CoV-2 infectivity and augments the inflammatory responses in airway epithelial cells. *Front. Immunol.* **2023**, *14*, 1112870. [CrossRef]
14. Hamming, I.; Timens, W.; Bulthuis, M.L.; Lely, A.T.; Navis, G.; van Goor, H. Tissue distribution of ACE2 protein, the functional receptor for SARS coronavirus. A first step in understanding SARS pathogenesis. *J. Pathol.* **2004**, *203*, 631–637. [CrossRef] [PubMed]
15. Iizuka, K.; Kusunoki, A.; Machida, T.; Hirafuji, M. Angiotensin II reduces membranous angiotensin-converting enzyme 2 in pressurized human aortic endothelial cells. *J. Renin Angiotensin Aldosterone Syst.* **2009**, *10*, 210–215. [CrossRef] [PubMed]
16. Zhao, Y.; Zhao, Z.; Wang, Y.; Zhou, Y.; Ma, Y.; Zuo, W. Single-Cell RNA Expression Profiling of ACE2, the Receptor of SARS-CoV-2. *Am. J. Respir. Crit. Care Med.* **2020**, *202*, 756–759. [CrossRef] [PubMed]
17. Perico, L.; Morigi, M.; Galbusera, M.; Pezzotta, A.; Gastoldi, S.; Imberti, B.; Perna, A.; Ruggenenti, P.; Donadelli, R.; Benigni, A.; et al. SARS-CoV-2 Spike Protein 1 Activates Microvascular Endothelial Cells and Complement System Leading to Platelet Aggregation. *Front. Immunol.* **2022**, *13*, 827146. [CrossRef] [PubMed]
18. George, S.; Pal, A.C.; Gagnon, J.; Timalsina, S.; Singh, P.; Vydyam, P.; Munshi, M.; Chiu, J.E.; Renard, I.; Harden, C.A.; et al. Evidence for SARS-CoV-2 Spike Protein in the Urine of COVID-19 Patients. *Kidney360* **2021**, *2*, 924–936. [CrossRef]
19. Veras, F.P.; Pontelli, M.C.; Silva, C.M.; Toller-Kawahisa, J.E.; de Lima, M.; Nascimento, D.C.; Schneider, A.H.; Caetite, D.; Tavares, L.A.; Paiva, I.M.; et al. SARS-CoV-2-triggered neutrophil extracellular traps mediate COVID-19 pathology. *J. Exp. Med.* **2020**, *217*, e20201129. [CrossRef] [PubMed]
20. Zuo, Y.; Yalavarthi, S.; Shi, H.; Gockman, K.; Zuo, M.; Madison, J.A.; Blair, C.; Weber, A.; Barnes, B.J.; Egeblad, M.; et al. Neutrophil extracellular traps in COVID-19. *JCI Insight* **2020**, *5*, e138999. [CrossRef]
21. Middleton, E.A.; He, X.Y.; Denorme, F.; Campbell, R.A.; Ng, D.; Salvatore, S.P.; Mostyka, M.; Baxter-Stoltzfus, A.; Borczuk, A.C.; Loda, M.; et al. Neutrophil extracellular traps contribute to immunothrombosis in COVID-19 acute respiratory distress syndrome. *Blood* **2020**, *136*, 1169–1179. [CrossRef]
22. Zuo, Y.; Zuo, M.; Yalavarthi, S.; Gockman, K.; Madison, J.A.; Shi, H.; Woodard, W.; Lezak, S.P.; Lugogo, N.L.; Knight, J.S.; et al. Neutrophil extracellular traps and thrombosis in COVID-19. *J. Thromb. Thrombolysis* **2020**, *51*, 446–453. [CrossRef]
23. Baugh, R.J.; Broze, G.J., Jr.; Krishnaswamy, S. Regulation of extrinsic pathway factor Xa formation by tissue factor pathway inhibitor. *J. Biol. Chem.* **1998**, *273*, 4378–4386. [CrossRef]
24. Bajaj, M.S.; Birktoft, J.J.; Steer, S.A.; Bajaj, S.P. Structure and biology of tissue factor pathway inhibitor. *Thromb. Haemost.* **2001**, *86*, 959–972. [PubMed]
25. Lwaleed, B.A.; Bass, P.S. Tissue factor pathway inhibitor: Structure, biology and involvement in disease. *J. Pathol.* **2006**, *208*, 327–339. [CrossRef] [PubMed]
26. Maroney, S.A.; Hansen, K.G.; Mast, A.E. Cellular expression and biological activities of alternatively spliced forms of tissue factor pathway inhibitor. *Curr. Opin. Hematol.* **2013**, *20*, 403–409. [CrossRef]
27. Loghmani, H.; Conway, E.M. Exploring traditional and nontraditional roles for thrombomodulin. *Blood* **2018**, *132*, 148–158. [CrossRef] [PubMed]
28. Wang, Y.; Li, M.; Stadler, S.; Correll, S.; Li, P.; Wang, D.; Hayama, R.; Leonelli, L.; Han, H.; Grigoryev, S.A.; et al. Histone hypercitrullination mediates chromatin decondensation and neutrophil extracellular trap formation. *J. Cell Biol.* **2009**, *184*, 205–213. [CrossRef] [PubMed]

29. Mauracher, L.M.; Posch, F.; Martinod, K.; Grilz, E.; Daullary, T.; Hell, L.; Brostjan, C.; Zielinski, C.; Ay, C.; Wagner, D.D.; et al. Citrullinated histone H3, a biomarker of neutrophil extracellular trap formation, predicts the risk of venous thromboembolism in cancer patients. *J. Thromb. Haemost.* **2018**, *16*, 508–518. [CrossRef]
30. Li, T.; Zhang, Z.; Li, X.; Dong, G.; Zhang, M.; Xu, Z.; Yang, J. Neutrophil Extracellular Traps: Signaling Properties and Disease Relevance. *Mediat. Inflamm.* **2020**, *2020*, 9254087. [CrossRef]
31. Fox, S.E.; Akmatbekov, A.; Harbert, J.L.; Li, G.; Quincy Brown, J.; Vander Heide, R.S. Pulmonary and cardiac pathology in African American patients with COVID-19: An autopsy series from New Orleans. *Lancet Respir. Med.* **2020**, *8*, 681–686. [CrossRef]
32. Barton, L.M.; Duval, E.J.; Stroberg, E.; Ghosh, S.; Mukhopadhyay, S. COVID-19 Autopsies, Oklahoma, USA. *Am. J. Clin. Pathol.* **2020**, *153*, 725–733. [CrossRef]
33. Hong, C.W. Current Understanding in Neutrophil Differentiation and Heterogeneity. *Immune Netw.* **2017**, *17*, 298–306. [CrossRef]
34. Jover, E.; Matilla, L.; Garaikoetxea, M.; Fernandez-Celis, A.; Muntendam, P.; Jaisser, F.; Rossignol, P.; Lopez-Andres, N. Beneficial Effects of Mineralocorticoid Receptor Pathway Blockade against Endothelial Inflammation Induced by SARS-CoV-2 Spike Protein. *Biomedicines* **2021**, *9*, 639. [CrossRef] [PubMed]
35. Patra, T.; Meyer, K.; Geerling, L.; Isbell, T.S.; Hoft, D.F.; Brien, J.; Pinto, A.K.; Ray, R.B.; Ray, R. SARS-CoV-2 spike protein promotes IL-6 trans-signaling by activation of angiotensin II receptor signaling in epithelial cells. *PLoS Pathog.* **2020**, *16*, e1009128. [CrossRef] [PubMed]
36. Khan, S.; Shafiei, M.S.; Longoria, C.; Schoggins, J.W.; Savani, R.C.; Zaki, H. SARS-CoV-2 spike protein induces inflammation via TLR2-dependent activation of the NF-kappaB pathway. *Elife* **2021**, *10*, e68563. [CrossRef]
37. Pantazi, I.; Al-Qahtani, A.A.; Alhamlan, F.S.; Alothaid, H.; Matou-Nasri, S.; Sourvinos, G.; Vergadi, E.; Tsatsanis, C. SARS-CoV-2/ACE2 Interaction Suppresses IRAK-M Expression and Promotes Pro-Inflammatory Cytokine Production in Macrophages. *Front. Immunol.* **2021**, *12*, 683800. [CrossRef]
38. Cao, X.; Tian, Y.; Nguyen, V.; Zhang, Y.; Gao, C.; Yin, R.; Carver, W.; Fan, D.; Albrecht, H.; Cui, T.; et al. Spike protein of SARS-CoV-2 activates macrophages and contributes to induction of acute lung inflammation in male mice. *FASEB J.* **2021**, *35*, e21801. [CrossRef] [PubMed]
39. Shirato, K.; Kizaki, T. SARS-CoV-2 spike protein S1 subunit induces pro-inflammatory responses via toll-like receptor 4 signaling in murine and human macrophages. *Heliyon* **2021**, *7*, e06187. [CrossRef]
40. Masso-Silva, J.A.; Moshensky, A.; Lam, M.T.Y.; Odish, M.F.; Patel, A.; Xu, L.; Hansen, E.; Trescott, S.; Nguyen, C.; Kim, R.; et al. Increased Peripheral Blood Neutrophil Activation Phenotypes and Neutrophil Extracellular Trap Formation in Critically Ill Coronavirus Disease 2019 (COVID-19) Patients: A Case Series and Review of the Literature. *Clin. Infect. Dis.* **2022**, *74*, 479–489. [CrossRef]
41. Patel, K.D.; Cuvelier, S.L.; Wiehler, S. Selectins: Critical mediators of leukocyte recruitment. *Semin. Immunol.* **2002**, *14*, 73–81. [CrossRef]
42. McEver, R.P. Selectins: Initiators of leucocyte adhesion and signalling at the vascular wall. *Cardiovasc. Res.* **2015**, *107*, 331–339. [CrossRef]
43. Lenting, P.J.; Christophe, O.D.; Denis, C.V. von Willebrand factor biosynthesis, secretion, and clearance: Connecting the far ends. *Blood* **2015**, *125*, 2019–2028. [CrossRef]
44. Vischer, U.M. von Willebrand factor, endothelial dysfunction, and cardiovascular disease. *J. Thromb. Haemost.* **2006**, *4*, 1186–1193. [CrossRef]
45. Chauhan, A.K.; Kisucka, J.; Lamb, C.B.; Bergmeier, W.; Wagner, D.D. von Willebrand factor and factor VIII are independently required to form stable occlusive thrombi in injured veins. *Blood* **2007**, *109*, 2424–2429. [CrossRef]
46. Bhargavan, B.; Kanmogne, G.D. SARS-CoV-2 Spike Proteins and Cell-Cell Communication Inhibits TFPI and Induces Thrombogenic Factors in Human Lung Microvascular Endothelial Cells and Neutrophils: Implications for COVID-19 Coagulopathy Pathogenesis. *Int. J. Mol. Sci.* **2022**, *23*, 10436. [CrossRef] [PubMed]
47. Goshua, G.; Pine, A.B.; Meizlish, M.L.; Chang, C.H.; Zhang, H.; Bahel, P.; Baluha, A.; Bar, N.; Bona, R.D.; Burns, A.J.; et al. Endotheliopathy in COVID-19-associated coagulopathy: Evidence from a single-centre, cross-sectional study. *Lancet Haematol.* **2020**, *7*, e575–e582. [CrossRef] [PubMed]
48. Pine, A.B.; Meizlish, M.L.; Goshua, G.; Chang, C.H.; Zhang, H.; Bishai, J.; Bahel, P.; Patel, A.; Gbyli, R.; Kwan, J.M.; et al. Circulating markers of angiogenesis and endotheliopathy in COVID-19. *Pulm. Circ.* **2020**, *10*, 2045894020966547. [CrossRef] [PubMed]
49. Iba, T.; Connors, J.M.; Levy, J.H. The coagulopathy, endotheliopathy, and vasculitis of COVID-19. *Inflamm. Res.* **2020**, *69*, 1181–1189. [CrossRef]
50. Kusunoki, Y.; Nakazawa, D.; Shida, H.; Hattanda, F.; Miyoshi, A.; Masuda, S.; Nishio, S.; Tomaru, U.; Atsumi, T.; Ishizu, A. Peptidylarginine Deiminase Inhibitor Suppresses Neutrophil Extracellular Trap Formation and MPO-ANCA Production. *Front. Immunol.* **2016**, *7*, 227. [CrossRef]
51. Rohrbach, A.S.; Slade, D.J.; Thompson, P.R.; Mowen, K.A. Activation of PAD4 in NET formation. *Front. Immunol.* **2012**, *3*, 360. [CrossRef]
52. Wong, S.L.; Wagner, D.D. Peptidylarginine deiminase 4: A nuclear button triggering neutrophil extracellular traps in inflammatory diseases and aging. *FASEB J.* **2018**, *32*, 6358–6370. [CrossRef]

53. Folco, E.J.; Mawson, T.L.; Vromman, A.; Bernardes-Souza, B.; Franck, G.; Persson, O.; Nakamura, M.; Newton, G.; Luscinskas, F.W.; Libby, P. Neutrophil Extracellular Traps Induce Endothelial Cell Activation and Tissue Factor Production Through Interleukin-1alpha and Cathepsin G. *Arterioscler. Thromb. Vasc. Biol.* **2018**, *38*, 1901–1912. [CrossRef]
54. Fuchs, T.A.; Brill, A.; Duerschmied, D.; Schatzberg, D.; Monestier, M.; Myers, D.D., Jr.; Wrobleski, S.K.; Wakefield, T.W.; Hartwig, J.H.; Wagner, D.D. Extracellular DNA traps promote thrombosis. *Proc. Natl. Acad. Sci. USA* **2010**, *107*, 15880–15885. [CrossRef] [PubMed]
55. Thalin, C.; Hisada, Y.; Lundstrom, S.; Mackman, N.; Wallen, H. Neutrophil Extracellular Traps: Villains and Targets in Arterial, Venous, and Cancer-Associated Thrombosis. *Arterioscler. Thromb. Vasc. Biol.* **2019**, *39*, 1724–1738. [CrossRef] [PubMed]
56. Longstaff, C.; Varju, I.; Sotonyi, P.; Szabo, L.; Krumrey, M.; Hoell, A.; Bota, A.; Varga, Z.; Komorowicz, E.; Kolev, K. Mechanical stability and fibrinolytic resistance of clots containing fibrin, DNA, and histones. *J. Biol. Chem.* **2013**, *288*, 6946–6956. [CrossRef] [PubMed]
57. Varju, I.; Longstaff, C.; Szabo, L.; Farkas, A.Z.; Varga-Szabo, V.J.; Tanka-Salamon, A.; Machovich, R.; Kolev, K. DNA, histones and neutrophil extracellular traps exert anti-fibrinolytic effects in a plasma environment. *Thromb. Haemost.* **2015**, *113*, 1289–1298. [CrossRef]
58. Saffarzadeh, M.; Juenemann, C.; Queisser, M.A.; Lochnit, G.; Barreto, G.; Galuska, S.P.; Lohmeyer, J.; Preissner, K.T. Neutrophil extracellular traps directly induce epithelial and endothelial cell death: A predominant role of histones. *PLoS ONE* **2012**, *7*, e32366. [CrossRef]
59. Carmona-Rivera, C.; Zhao, W.; Yalavarthi, S.; Kaplan, M.J. Neutrophil extracellular traps induce endothelial dysfunction in systemic lupus erythematosus through the activation of matrix metalloproteinase-2. *Ann. Rheum. Dis.* **2015**, *74*, 1417–1424. [CrossRef] [PubMed]
60. Rabinovitch, M. NETs Activate Pulmonary Arterial Endothelial Cells. *Arterioscler. Thromb. Vasc. Biol.* **2016**, *36*, 2035–2037. [CrossRef]
61. Dubey, A.; Choudhary, S.; Kumar, P.; Tomar, S. Emerging SARS-CoV-2 Variants: Genetic Variability and Clinical Implications. *Curr. Microbiol.* **2021**, *79*, 20. [CrossRef]
62. Boehm, E.; Kronig, I.; Neher, R.A.; Eckerle, I.; Vetter, P.; Kaiser, L.; Geneva Centre for Emerging Viral, D. Novel SARS-CoV-2 variants: The pandemics within the pandemic. *Clin. Microbiol. Infect.* **2021**, *27*, 1109–1117. [CrossRef]
63. Singh, J.; Pandit, P.; McArthur, A.G.; Banerjee, A.; Mossman, K. Evolutionary trajectory of SARS-CoV-2 and emerging variants. *Virol. J.* **2021**, *18*, 166. [CrossRef]
64. Broze, G.J., Jr.; Girard, T.J. Tissue factor pathway inhibitor: Structure-function. *Front. Biosci.* **2012**, *17*, 262–280. [CrossRef] [PubMed]
65. Ellery, P.E.; Adams, M.J. Tissue factor pathway inhibitor: Then and now. *Semin. Thromb. Hemost.* **2014**, *40*, 881–886. [CrossRef] [PubMed]
66. Mast, A.E. Tissue Factor Pathway Inhibitor: Multiple Anticoagulant Activities for a Single Protein. *Arterioscler. Thromb. Vasc. Biol.* **2016**, *36*, 9–14. [CrossRef] [PubMed]
67. Chen, V.M. Tissue factor de-encryption, thrombus formation, and thiol-disulfide exchange. *Semin. Thromb. Hemost.* **2013**, *39*, 40–47. [CrossRef]
68. Chen, V.M.; Ahamed, J.; Versteeg, H.H.; Berndt, M.C.; Ruf, W.; Hogg, P.J. Evidence for activation of tissue factor by an allosteric disulfide bond. *Biochemistry* **2006**, *45*, 12020–12028. [CrossRef]
69. Prasad, R.; Banerjee, S.; Sen, P. Contribution of allosteric disulfide in the structural regulation of membrane-bound tissue factor-factor VIIa binary complex. *J. Biomol. Struct. Dyn.* **2019**, *37*, 3707–3720. [CrossRef]
70. Winther, J.R.; Thorpe, C. Quantification of thiols and disulfides. *Biochim. Biophys. Acta* **2014**, *1840*, 838–846. [CrossRef]
71. Khanna, K.; Raymond, W.; Jin, J.; Charbit, A.R.; Gitlin, I.; Tang, M.; Werts, A.D.; Barrett, E.G.; Cox, J.M.; Birch, S.M.; et al. Thiol drugs decrease SARS-CoV-2 lung injury in vivo and disrupt SARS-CoV-2 spike complex binding to ACE2 in vitro. *bioRxiv* **2021**. [CrossRef]
72. Khanna, K.; Raymond, W.W.; Jin, J.; Charbit, A.R.; Gitlin, I.; Tang, M.; Werts, A.D.; Barrett, E.G.; Cox, J.M.; Birch, S.M.; et al. Exploring antiviral and anti-inflammatory effects of thiol drugs in COVID-19. *Am. J. Physiol. Lung Cell. Mol. Physiol.* **2022**, *323*, L372–L389. [CrossRef]
73. Wu, X.; Xiang, M.; Jing, H.; Wang, C.; Novakovic, V.A.; Shi, J. Damage to endothelial barriers and its contribution to long COVID. *Angiogenesis* **2023**, 1–18. [CrossRef]
74. Liu, R.; Pan, J.; Zhang, C.; Sun, X. Cardiovascular Complications of COVID-19 Vaccines. *Front. Cardiovasc. Med.* **2022**, *9*, 840929. [CrossRef] [PubMed]
75. Ostrowski, S.R.; Sogaard, O.S.; Tolstrup, M.; Staerke, N.B.; Lundgren, J.; Ostergaard, L.; Hvas, A.M. Inflammation and Platelet Activation After COVID-19 Vaccines—Possible Mechanisms Behind Vaccine-Induced Immune Thrombocytopenia and Thrombosis. *Front. Immunol.* **2021**, *12*, 779453. [CrossRef] [PubMed]
76. Chang, J.C.; Hawley, H.B. Vaccine-Associated Thrombocytopenia and Thrombosis: Venous Endotheliopathy Leading to Venous Combined Micro-Macrothrombosis. *Medicina* **2021**, *57*, 1163. [CrossRef]
77. Colunga Biancatelli, R.M.L.; Solopov, P.A.; Sharlow, E.R.; Lazo, J.S.; Marik, P.E.; Catravas, J.D. The SARS-CoV-2 spike protein subunit S1 induces COVID-19-like acute lung injury in Kappa18-hACE2 transgenic mice and barrier dysfunction in human endothelial cells. *Am. J. Physiol. Lung Cell. Mol. Physiol.* **2021**, *321*, L477–L484. [CrossRef] [PubMed]

78. Kanmogne, G.D.; Kennedy, R.C.; Grammas, P. Analysis of human lung endothelial cells for susceptibility to HIV type 1 infection, coreceptor expression, and cytotoxicity of gp120 protein. *AIDS Res. Hum. Retroviruses* **2001**, *17*, 45–53. [CrossRef] [PubMed]
79. Kanmogne, G.D.; Primeaux, C.; Grammas, P. Induction of apoptosis and endothelin-1 secretion in primary human lung endothelial cells by HIV-1 gp120 proteins. *Biochem. Biophys. Res. Commun.* **2005**, *333*, 1107–1115. [CrossRef]
80. Li, H.; Singh, S.; Potula, R.; Persidsky, Y.; Kanmogne, G.D. Dysregulation of claudin-5 in HIV-induced interstitial pneumonitis and lung vascular injury. Protective role of peroxisome proliferator-activated receptor-gamma. *Am. J. Respir. Crit. Care Med.* **2014**, *190*, 85–97. [CrossRef]
81. Woollard, S.M.; Li, H.; Singh, S.; Yu, F.; Kanmogne, G.D. HIV-1 induces cytoskeletal alterations and Rac1 activation during monocyte-blood-brain barrier interactions: Modulatory role of CCR5. *Retrovirology* **2014**, *11*, 20. [CrossRef]
82. Cui, X.Y.; Tjonnfjord, G.E.; Kanse, S.M.; Dahm, A.E.A.; Iversen, N.; Myklebust, C.F.; Sun, L.; Jiang, Z.X.; Ueland, T.; Campbell, J.J.; et al. Tissue factor pathway inhibitor upregulates CXCR7 expression and enhances CXCL12-mediated migration in chronic lymphocytic leukemia. *Sci. Rep.* **2021**, *11*, 5127. [CrossRef]
83. Chaudhuri, A.; Yang, B.; Gendelman, H.E.; Persidsky, Y.; Kanmogne, G.D. STAT1 signaling modulates HIV-1-induced inflammatory responses and leukocyte transmigration across the blood-brain barrier. *Blood* **2008**, *111*, 2062–2072. [CrossRef]
84. Bhargavan, B.; Kanmogne, G.D. Toll-Like Receptor-3 Mediates HIV-1-Induced Interleukin-6 Expression in the Human Brain Endothelium via TAK1 and JNK Pathways: Implications for Viral Neuropathogenesis. *Mol. Neurobiol.* **2018**, *55*, 5976–5992. [CrossRef] [PubMed]
85. Bhargavan, B.; Woollard, S.M.; McMillan, J.E.; Kanmogne, G.D. CCR5 antagonist reduces HIV-induced amyloidogenesis, tau pathology, neurodegeneration, and blood-brain barrier alterations in HIV-infected hu-PBL-NSG mice. *Mol. Neurodegener.* **2021**, *16*, 78. [CrossRef] [PubMed]
86. Bhargavan, B.; Woollard, S.M.; Kanmogne, G.D. Toll-like receptor-3 mediates HIV-1 transactivation via NFκB and JNK pathways and histone acetylation, but prolonged activation suppresses Tat and HIV-1 replication. *Cell. Signal.* **2016**, *28*, 7–22. [CrossRef] [PubMed]